Advances in Science and Technology Research Journal

Volume 14, Issue 1, March 2020, pages 127–136
https://doi.org/10.12913/22998624/114029

Received: 2019.10.12
Revised: 2020.01.10
Accepted: 2020.02.04
Available online: 2020.02.14

Numerical Modeling of Superplastic Punchless Deep Drawing Process of a TI-6AL-4V Titanium Alloy

Andrzej Skrzat[1], Marta Wójcik[1*]

[1] Department of Materials Forming and Processing, Rzeszow University of Technology, Al. Powstańców Warszawy 8, 35-959 Rzeszów, Poland

* Corresponding author's e-mail: m.wojcik@prz.edu.pl

ABSTRACT

The numerical results of superplastic punchless deep drawing of the Ti-6Al-4V titanium alloy were presented in this paper. The material behavior subjected to the forming process was characterized by deformation-microstructure constitutive equations including the grain growth. Superplastic stress-strain characteristics used in the numerical simulations were computed with the application of authorial program. The explicit integration scheme is used in solving differential equations. The numerical simulations of the super-elastic deep drawing were made with finite element method analysis. The von Mises stress distribution in the blow-forming process was obtained. The possible faults of extrusions caused by the improper load history as well as unsuitable pressure were also presented in this paper. The numerical simulations included in this research allow for the proper choice of material and drawing parameters which can help to optimize the superplastic forming process.

Keywords: superplastic forming process, superplasticity, Ti-6Al-4V titanium alloy, blow forming, deep drawing, viscoplasticity

INTRODUCTION

The Ti-6Al-4V titanium alloy (UNS R56400 or Grade 5) is a kind of an α/β alloy which is useful in various branches of manufacture, including the aerospace industry, for the production of e.g. fan blades and airframes [1, 12]. The main advantages of the Ti-6Al-4V alloy, which determines its wide application in the industry sector, are a high mechanical strength, high working temperatures as well as a good welding performance [9, 47, 48]. These mechanical properties of the Ti-6Al-4V alloy might cause difficulties in forming at room temperature [43]. The superplastic forming process is an alternative advanced manufacturing method for the fabrication of complex-shape parts made of titanium and other alloys which indicate the superplastic state under certain conditions.

Superplasticity is an ability to undergo large plastic deformation exceeding 200% without necking and failing at relatively low stresses (Fig. 1) [8]. Typically, the elongations from 200 to 1000% can be achieved in the superplastic state. Superplasticity, as the highly strain-rate dependent, nonlinear viscous behavior of materials, occurs in many metals, alloys, ceramics and intermetallic materials with fine structure, e.g. in aluminum or titanium alloys [3, 7, 42].

Special conditions are essential to achieve the superplastic elongation in the tensile test. The superplastic forming process occurs in fine-grained materials with an average grain size usually lesser than 10-15 μm for metals and below 1 μm for ceramics in high homologous temperature exceeding 0.5 T_m, where T_m is an absolute melting point [31]. The superplastic materials are also characterized by the low flow stress <10 MPa and high uniformity of the plastic flow [15].

The superplastic forming process usually occurs in the controlled low strain rate at the range of $10^{-4} – 10^{-2}$ s^{-1}. The superplasticity might also arise in high strain rates even $>10^4$ s^{-1} *(high strain-rate superplasticity)* [16, 28]. The aforementioned

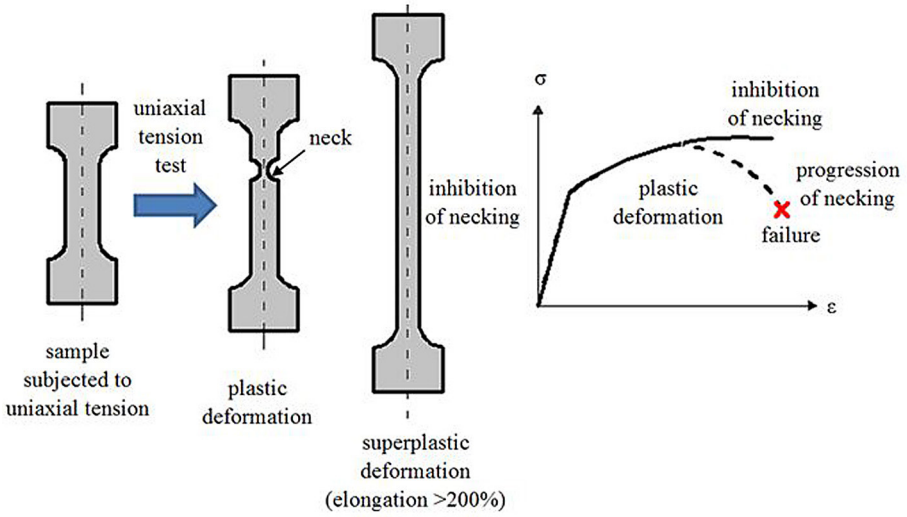

Fig. 1. Differences between plastic and superplastic elongations

conditions allow the superplastic behavior of a material to be defined [18] as a complex function of the strain rate $(\dot{\varepsilon})$, strain (ε), temperature (T) and the grain size (d) (Eq. 1)

$$\sigma = f(\dot{\varepsilon}, \varepsilon, T, d) \tag{1}$$

The strain rate is inversely proportional to the grain size [36, 37] in line with Eq. 2

$$\dot{\varepsilon} = \alpha \cdot d^{-p} \tag{2}$$

where: α is a material constant,
d is an average grain size and
p is a grain growth exponent which characterizes the deformation micromechanism. Usually, one assumes that p=2 or p=3.

The abovementioned requirements enable to distinguish fine-structure superplasticity (FSS) which occurs in the materials with an average grain size < 15 μm and internal-stress superplasticity (ISS) caused by special external conditions, e.g. pressure or thermal activity [40].

The superplasticity phenomenon has been the subject of research for years. The first laboratory research concerning the superplastic deformation was carried out by Bengough in 1912 who obtained the elongation of 163% in α/β brass at 427 K [41]. Sherby [39] speculates that the ancient bronzes (2500 BC) and Damascus steel (350 BC) probably indicated the superplastic behavior. In the first half of the 20th century, the superplastic deformation of different materials was also examined by Jenkins (1928) and Pearson (1934) [10, 19]. The main aim of their research was to obtain the highest elongation in uniaxial tensile tests. After 1945, the papers on the superplasticity phenomenon have appeared occasionally. The major increase in the interest of superplasticity was noted from 1962 onwards [13, 28]. In 1967, Lee and Backofen achieved the elongation of >1000% for Ti-6wt%Al-4wt%V (Ti-6/4) [37]. The superplasticity phenomenon in a magnesium alloy subjected to isothermal rolling was described in [11]. The 1100% elongation was achieved in this research. The superplastic behavior of the friction stir welded Ti-6Al-4V joint at 454 K and for $\dot{\varepsilon} = 3 \cdot 10^{-4} - 1 \cdot 10^{-3}$ s^{-1} was examined in [46]. The microstructure and superplasticity of Al-Cu-Y-Zr alloy within temperature in the range of 277-307 K and the strain rate range of $10^{-4} - 10^{-3}$ s^{-1} was also investigated in [32]. The superplasticity of the nano-grained Mg-Gd-Y-Zr alloy at temperatures of 573-723 K under strain rates in the range of $3.3 \cdot 10^{-3} - 2.7 \cdot 10^{-1}$ s^{-1} was analyzed in [2].

The superplasticity phenomenon has also been a subject of research carried out on a technical scale. In 1964, Backofen et al. showed that the Zn-Al alloy could be formed into a hemispherical shape by blowing air on one side of a sheet into a die [35]. It was considered as the first investigation of superplastic forming on a technical scale. The application of superplastic forming for fabrication of structural components made from the magnesium alloy is described in [26].

In recent years, the modeling of superplastic forming has been widely used in order to optimize the process on a technical scale. Lin and Dunne [20] modelled the evolution of grain growth and the necking in the superplastic blow-forming

process of titanium alloy. In [29], the modelling of failure and stability of different alloys during the superplastic deformation was presented. The results of numerical simulations of the superplastic forming process of the Ti-6Al-4V titanium alloy are found in [27]. The experimental research and numerical simulations of superplastic forming of the Ti-6Al-4V titanium alloy at different strain rates and in different temperatures are presented in [24, 25]. The results of numerical simulations of the high strain rate superplastic forming of the Al-6Mg-0.2Sc alloy are contained in [5]. The numerical simulations of superplastic forming of dental and medical prostheses are presented in [4].

The aim of this paper was the numerical analysis of superplastic behavior of the Ti-6Al-4V titanium alloy subjected to a uniaxial tension test at 655 K for strain rate at the range of $10^{-4} - 10^{-3}$ s^{-1}. Firstly, the superplastic material response was analyzed and the authorial program simulating the uniaxial tension test for the Ti-6Al-4V titanium alloy based on the superplastic model proposed by Dunne and Petrinic [8] was developed. Then, the stress-strain curves for various strain rates were introduced to the commercial ABAQUS program. Finally, the punch less superplastic deep drawing process was analyzed. Different load histories and pressure values were investigated in the numerical simulations. The influence of process parameters on the shape and quality of an extrusion was examined.

CONSTITUTIVE EQUATIONS OF SUPERPLASTICITY

During the uniaxial tension test, the material in the superplastic state deformed viscoplastically. The mechanical properties of the material in the superplastic state were represented by viscous liquid models. Most material viscoplastic models are usually defined by the relationship between the second invariants of the deviator of the Cauchy stress tensor and the strain-rate tensor [31].

Numerous phenomenological and physical constitutive equations were proposed to describe the material flow stress response. In the superplastic regime, the relationship between the strain rate and the flow stress for the one dimensional problem might be simply described with the use of an equation proposed by Backofen et al. (Eq. 3)[33].

$$\sigma = K\,\dot{\varepsilon}^{m} \tag{3}$$

Rearranging Eq. 3 gives

$$\dot{\varepsilon} = C\,\sigma^{n} \tag{4}$$

where: $C = \frac{1}{K^{1/m}}$ and $n = \frac{1}{m}$.

After ln-transformation

$$\ln(\sigma) = m\ln(\dot{\varepsilon}) + k \tag{5}$$

where: σ is the true flow stress,
$\dot{\varepsilon}$ is the strain rate,
K and k are material constants depending on testing conditions
and m is the strain-rate sensitivity.

In logarithmic coordinates, the relationship $\ln(\sigma) - \ln(\dot{\varepsilon})$ is approximately a straight line for a small strain rate interval, with the slope equal to m.

The strain-rate sensitivity is described by Eq. 6 [33, 34]:

$$m = \frac{\partial \ln(\sigma)}{\partial \ln(\dot{\varepsilon})} \tag{6}$$

The $\ln(\sigma) - \ln(\dot{\varepsilon})$ as well as $\mathrm{m} - \ln(\dot{\varepsilon})$ relationships are shown in Fig. 2. The shape of $\ln(\sigma) - \ln(\dot{\varepsilon})$ curve is sigmoidal and the $\mathrm{m} - \ln(\dot{\varepsilon})$ curve has a dome-like shape for which the maximum m value corresponds to the optimal strain rate in a superplastic regime for the given average grain size and the given temperature. The optimal strain rate interval is indicated from an empirical condition $m \geq 0.3$ [33]. For the majority of superplastic materials, *m* is in the range of 0.4-0.8 [34]. Higher values of the strain-rate sensitivity mean better superplastic elongation without necking and failing.

Eq. 3 does not consider the strain hardening which might occur during superplastic forming. The isothermal, near-constant grain size, stress-strain rate relationship including isotropic hardening in a superplastic state is described by means of Norton-Hoff power law (Eq. 7) [14, 30].

$$\sigma = K\,\varepsilon^{n}\,\dot{\varepsilon}^{m} \tag{7}$$

where *n* is an isotropic exponent.

Equations (3) and (7) are commonly applied to describe the superplasticity phenomenon but they are inadequate for simulating the superplastic forming because they do not consider the change of the microstructure. Additionally, the $\ln(\sigma) - \ln(\dot{\varepsilon})$ relationship might be nonlinear [38].

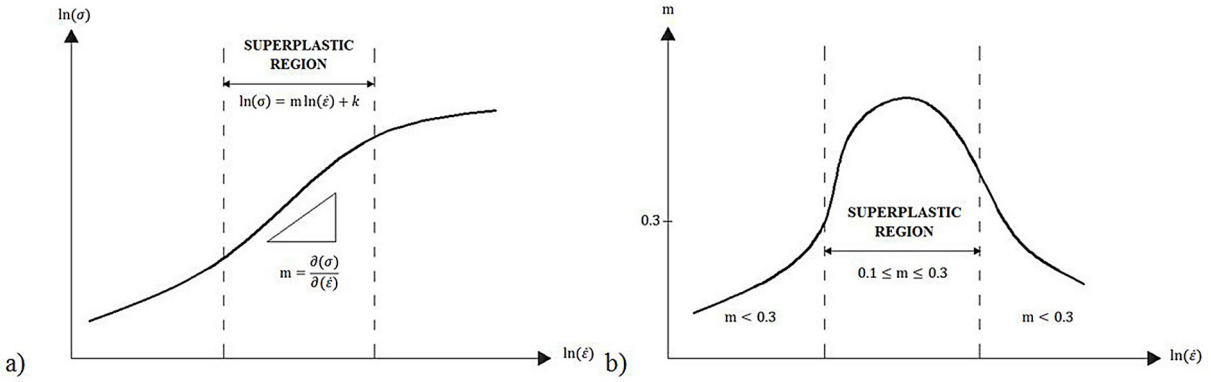

Fig. 2. The relationship $\ln(\sigma) - \ln(\dot{\varepsilon})$ (a) and $\mathrm{m} - \ln(\dot{\varepsilon})$ for superplastic deformation (b)

Recently, more advanced formulations for describing the superplastic forming have been proposed, including the stress-strain, stress-strain rate behavior and furthermore, the dependence of the strain rate sensitivity on the strain rate and average grain size (Tab. 1). These models can also describe the strain hardening caused by the static and dynamic growth as well as the evolution of an average grain size. Deformation-microstructure constitutive equations can be found in [6, 17, 21, 22, 24, 25]. The application of complex superplastic models requires the knowledge of the material data usually designated in the experimental tests.

The superplastic model proposed by Dunne and Petrinic [8, 20] was used in this research. This model was formulated as the set of

Table 1. Constitutive equations for superplastic metals [22, 23]

Model	Equation	Parameters and Constants	Information about the model
Power law	$\sigma = K\,\varepsilon^n \dot{\varepsilon}^m$	K, n and m	– the model parameters can be easily determined – does not take into account material softening and damage
Sinh law	$\dot{\varepsilon} = A\,(\sinh(\alpha\sigma))^{1/m}$	A, α and m	– the model parameters can be defined simply – does not take into account microstructural changes and material softening and damage
Unified constitutive model	$\dot{\varepsilon}_p = \left(\frac{(\lvert\sigma - X\rvert - r - k)}{K}\right)^{1/m} d^{-u}$ $\dot{X} = C\dot{\varepsilon}_p - \gamma X\lvert\dot{\varepsilon}_p\rvert$ $\dot{R} = b(Q - R)\lvert\dot{\varepsilon}_p\rvert$ $\dot{d} = (\alpha + \beta\lvert\dot{\varepsilon}_p\rvert)d^{-\gamma_0}$ $\sigma = E(\varepsilon_T - \varepsilon_p)$	E, K, k, u, C, γ, b, Q, α, β, γ_0 and m	– takes into account both hardening and softening, as well as the grain size evolution – solving the equations requires special numerical operations – determining the model parameters and material constants requires several experiments and advanced numerical operations
Simplified microstructure-based overstress model	$\dot{\varepsilon}_p = \frac{C_3\left(\frac{\sigma}{1 - f_0}\right)^{1/m}}{d^p}$ $d = d_0 + C_4\varepsilon$ $f_a = f_0 \exp(\varphi\sigma)$	C_3, C_4, f_0, φ, d_0, p, and m	– a simplified version of the microstructure-based overstress model – the grain growth (d) and damage accumulations are considered in the model – strain hardening and softening may not be accurately captured (due to simplifications)
Majidi et al. model	$\sigma = exp(\frac{1}{2}g(\varepsilon_p)ln^2(\varepsilon_p) + (h(\varepsilon_p) + m_0)ln(\dot{\varepsilon}_p) + m_1)$ $g(\varepsilon_p) = g_1 + g_2\varepsilon_p$ $h(\varepsilon_p) = h_1(\varepsilon_p + h_2)^{h_3} + h_4\varepsilon_p$	m_0, m_1, h_1, h_2, h_3, h_4, g_1 and g_2	– m-values might be calculated from the true stress-plastic strain curves of a material and the cavitation parameters, *f0* and *φ* might be obtained from micrography research, – other parameters are obtained from numerical calculations

elastic-viscoplastic constitutive equations representing the material behavior during the superplastic forming at different strain rates. The essential feature of this model is the consideration of the microstructure change related to the grain size growth. The model proposed by Dunne and Petrinic [8] in one-dimensional case is defined by the following equations:

- the sinh-law based viscoplastic constitutive equation

$$\dot{\varepsilon}^p = \frac{\propto}{l^\mu} sinh\, \beta(\sigma - r - \sigma_y) \tag{8}$$

where: $\dot{\varepsilon}^p$ is the plastic strain rate, $\propto and\ \beta$ are material constants, r is an isotropic hardening variable and μ is the deformation-microstructure coupling constant.

- the isotropic hardening

$$\dot{r} = (c_1 - \gamma_1 r)\dot{p} \tag{9}$$

where: c_1 and γ_1 are material constants and $\dot{p}$ is the effective plastic strain.

- the Hooke's law

$$\dot{\sigma} = E(\dot{\varepsilon} - \dot{\varepsilon}^p) \tag{10}$$

The change of microstructure of material is related with an increase of a grain size. The deformation-enhanced grain growth can be written as:

$$\dot{l} = \frac{\alpha_1}{l^\mu} + \beta_1 \dot{p} \tag{11}$$

where: c_1, γ_1, β_1 and μ are material constants and l is an average grain size.

An original numerical program based on the explicit integration of (8)-(11) equations was developed. The material constants appointed by Dunne and Petrinic [8] were used as shown in Table 2.

It is worth noting that the solution of equations (8-11) might be an ill-conditioned problem – see the magnitudes of α_1 and β_1 parameters. It is also very important for the convergence that parameter l must be expressed in μm.

On the basis of the superplastic model proposed in [5], the numerical program was developed. In the explicit integration of the constitutive equations (8)-(11) the stress-strain curves for a Ti-6Al-4V titanium alloy for various strain rates were generated.

The stress vs. strain curves for strain rates of $10^{-2} - 10^{2}$ s^{-1} are presented in Figure 3. One can see that the yield stress increases along with the strain rate which is an important feature of materials in a superplastic state.

Numerically generates stress-plastic strain curves were used later on as material characteristics in simulations of the superplastic deep drawing process.

SIMULATION OF SUPERPLASTIC DEEP DRAWING

The finite element simulation for superplastic deep drawing of a cylindrical extrusion made from the Ti-6Al-4V titanium alloy at 655 K was carried out using the commercial ABAQUS program. In this research, the superplastic deep-drawing was solved as 3D analysis using the explicit dynamic procedure.

The model of the punchless superplastic deep drawing consists of the die, the blank holder and the flat metal alloy sheet which is subjected to the pressure in order to achieve the die shape. The metal sheet was modeled as a deformable body and all tools were considered as analytical rigid bodies. Such an approach enables to shorten the analysis time, unless the shape of the tools is relatively simple. Analytical rigid bodies do not require generation of finite element mesh, which decreases the size of the problem. The general view of the model is shown in Figure 4.

In this research, the sheet made from Ti-6Al-4V was a flat blank with $5.4 \cdot 10^{-2}$ m diameter and uniform thickness of 10^{-3} m. The metal

Table 2. Material constants used in numerical simulations

Material constants	Value
α [-]	$0.437 \cdot 10^{-5}$
β [-]	0.0919
μ [-]	1.06
σ_y [MPa]	0.5
E [MPa]	1000
l [μm]	6.4
c_1[-]	8.397
α_1[-]	$0.128 \cdot 10^{-16}$
β_1[-]	$0.9625 \cdot 10^{-13}$
γ_1[-]	0.666
γ[-]	5.0

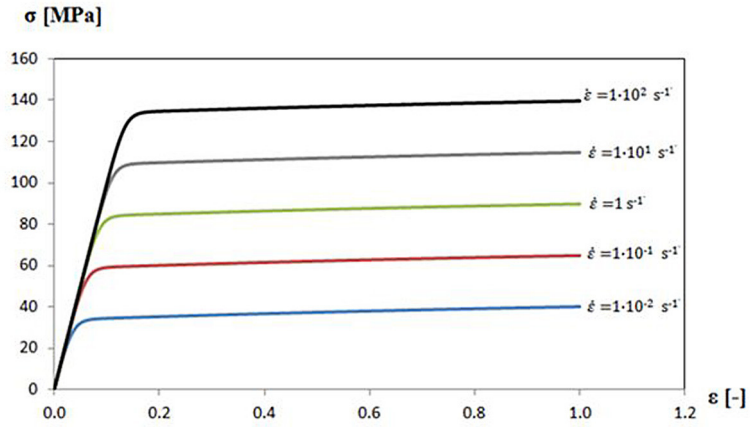

Figure 3. Numerically generated stress- strain curves for a Ti-6Al-4V titanium alloy at 655 K for strain rates of $10^{-2} - 10^{2}$ s^{-1}

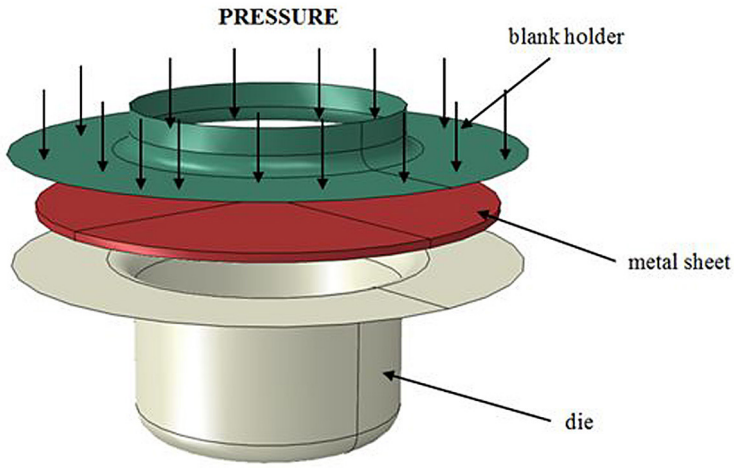

Figure 4. The assembly of superplastic forming process

sheet was discretized by 11088 C3D8R eight-nodes brick elements with linear shape function. Reduced integration was used to avoid the locking effects. The die and the blank holder were fixed by the applied boundary conditions. The following material data for the Ti-6Al-4V alloy sheet were used: density – 4.5 kg/m^3, Young's modulus – 100 MPa, Poisson's ratio – 0.3. The friction between metal sheet and tools was described by means of Coulomb friction model with a friction coefficient of 0.135.

The details of used numerical model are contained in Table 3. The pressure applied to the top of the metal sheet was in the range of 5-10 MPa. The numerical simulations were carried out for various strain rates of $10^{-2} - 10^{2}$ s^{-1}. The problem was solved in the single step consisting of approximately ten thousand increments. The stable time increment was about $7 \cdot 10^{-7}$ (explicit integration is conditionally stable).

Table 3. Details of the numerical model

Feature	Description
Numerical model	3D
Material model	elastic-viscoplastic
Integration procedure	dynamic explicit
Friction formulation	penalty
Friction coefficient	Coulomb model – 0.135
Tool's type	analytical body
Steps	1 step – blast press
Step time	0.007 s
Number of elements	11 088
Type of elements	C3D8R (continuous, 3-dimensional, 8-nodes, reduced integration)
Stable time increment	8·10^{-7} s

ANALYSIS RESULTS

Many numerical simulations of superplastic punchless deep drawing process for various pressure values and load histories were executed. The following parameters influencing the quality of the drawpiece were investigated:

- the magnitude of the pressure applied,
- the history of the load applied (the rate of the pressure applied, the time of the pressure saturation),
- the springback phenomenon after the superplastic forming,
- the type of elements used to model titanium sheet, i.e. continuous 3D elements vs. shell elements,
- the possibility of the mass scaling on order to decrease the computation time.

The selected results obtained in this research program are presented below.

Figure. 5 presents the distribution of the von Mises stress in the metal sheet after superplastic deep drawing for the pressures applied: 5, 8 and 10 MPa. It can be seen that the stresses are not uniformly distributed over the sheet. Similar non-uniform distribution can be observed for effective plastic strains (Fig. 6). The highest value of stress occurs in the neighborhood of the extrusion's collar. Additionally, the numerical analysis indicates that the bottom roundings are fully formed at the end of the process (see Fig. 6).

The value of the pressure applied has significant influence on the extrusion shape after the superplastic deep drawing process (see Fig. 5). The overstated pressure results in the presence of folding walls.

The load history influences on the distribution of strain in a metal sheet as well as the quality of the extrusion (Fig. 8). The results presented in Figure 7 show that inappropriate pressure history can cause drawpiece folds.

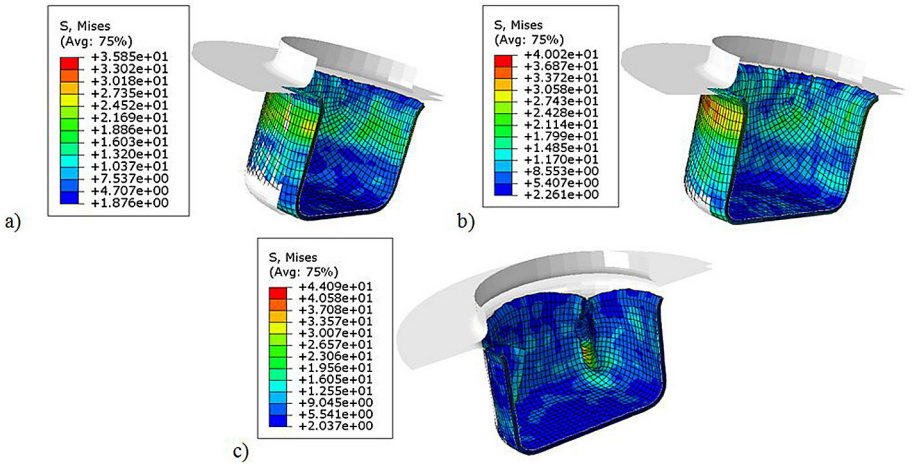

Figure 5. Distribution of the von Misses stress in Ti-6Al-4V titanium alloy sheet for 5 (a), 8 (b) and 10 (c) MPa pressure values

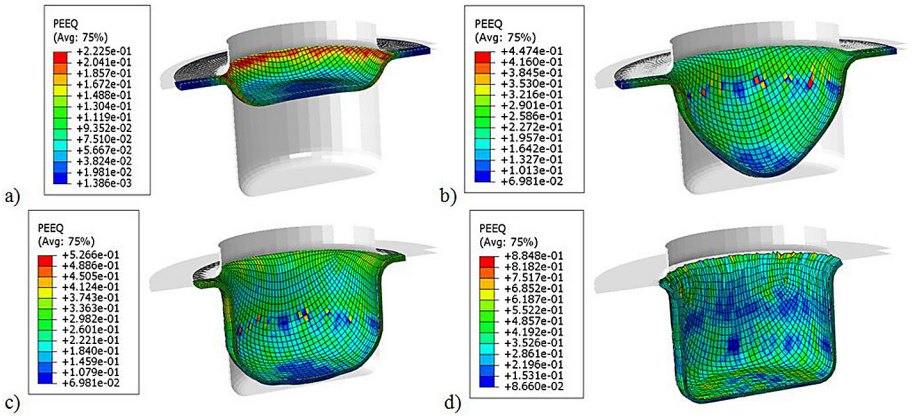

Figure 6. Effective plastic strains at time $t = 0.06$ (a), $t = 0.1$ (b), $t = 0.2$ (c) and $t = 1.0$ s (d)

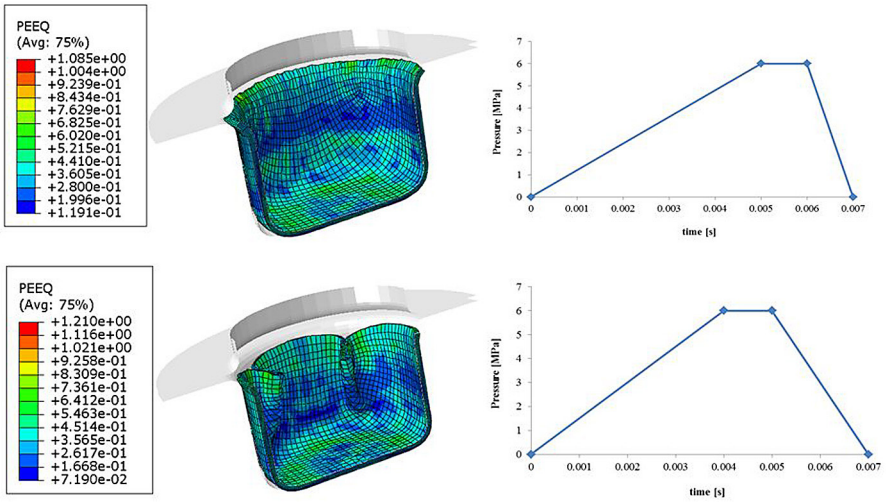

Fig. 7. The distribution of effective plastic strain in extrusions after superplastic forming for different load histories (pressure 6 MPa)

During the deep drawing process, deviations in the dimensions of the final product got springback effect. This elastic recovery of material occurring after the tool is removed or released, depends on the material properties as well as the process parameters, e.g. friction contact condition and punch or blankholder force [44, 45]. Numerical modeling of the deep drawing process might predict the springback effect in the deformed sheet and enables to obtain the part with a desirable shape. An exemplary springback effect which occurs in a superplastic deep drawing process is shown in Figure 8.

CONCLUSIONS

Numerical modeling of punchless deep drawing process in a superplastic regime was presented in this research. The Ti-6Al-4V titanium alloy material model introduced by Dunne and Petrinic was used in the analysis. Constitutive equations used in this material model included both deformation and the microstructure change related to the grain size growth.

On the basis of the model proposed by Dunne and Petrinic, an original program simulating the uniaxial tension test for the Ti-6Al-4V titanium alloy at a temperature of 655 K was developed. The numerically generated stress-strain curves for strain rates of $10^{-2} - 10^{2}$ s^{-1} are obtained by the explicit integration of the constitutive equations. Later on, they are applied in the simulations of the superplastic deep drawing process in commercial ABAQUS program. The process was modeled as 3D analysis using explicit dynamic procedure. The metal sheet was discretized by means of 11088 C3D8R eight-nodes brick elements with linear shape function in order to avoid the locking effects.

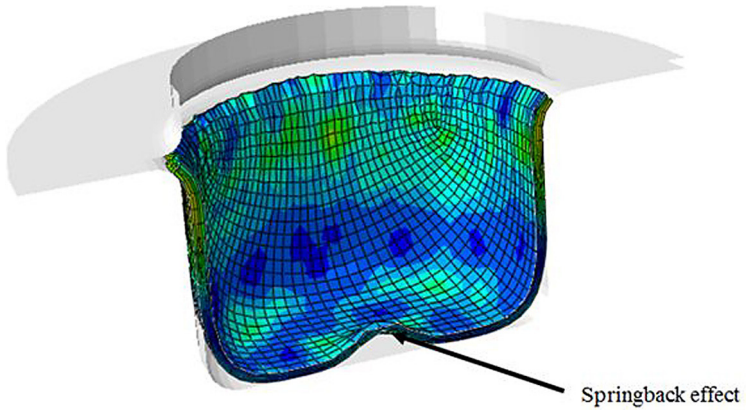

Fig. 8. The springback phenomenon for Ti-6Al-4V during the superplastic forming

Many numerical simulations for various pressure values as well as load histories were performed in this paper. Numerical tests showed that the pressure value applied in a forming process as well as the load history influence the quality of the extrusion obtained. Even a small change in the process parameters results in different distribution of stress or equivalent plastic strain in an extrusion and hence the shape of the extrusion obtained. Additionally, the improper choice of load history might result in the folding of an extrusion's collar. Numerical analysis also allows the springback effect investigation in the superplastic deep drawing process. The precise prediction of springback phenomenon is very important in the sheet metal forming processes and helps in the design of tools as well as provides the correct shape of the formed parts.

The research contained in this paper shows that it is possible to use the finite element method to design the deep drawing process leads to the reduction of extrusion's faults or springback effect. Numerical simulations of superplastic forming enable to optimize the process and select the optimal shape of tools in order to decrease their wearing. This will reduce the cost of development of the deep drawing instrumentation when compared to the prototype preparation and experimental investigations.

REFERENCES

1. Adamus J., Winowiecka J., Dyner M., Lacki P. Numerical simulation of forming titanium thin-wall panels with stiffeners. Advances in Science and Technology Research Journal, 12(1), 2018, 54-62.
2. Alizadeh R., Mahmudi R., Ngan A.H.W., Huang Y. and Langdon T.G. Superplasticity of a nano-grained Mg-Gd-Y-Zr alloy processed by high-pressure torsion. Materials Science and Engineering A, 651, 2016, 786-794.
3. Berdichevskij E.G. Use of the superplasticity effect of materials in engineering technology. IOP Conference Series: Materials Science and Engineering, 441, 2018, 1-5.
4. Bonet J., Wood R.D., Said R., Curtis R.V. and Garriga-Majo D. Numerical simulation of the superplastic forming of dental and medical prostheses. Biomechanics and Modeling in Mechanobiology, 1(3), 2002, 177-196.
5. Chen M. H., Xue Y.H., Rui Y.L., Zhou J.H. and Wang M. Numerical Simulation and Experimental Investigation of High Strain Rate Superplastic Forming (SPF) of Al-6Mg-0.2Sc Alloy. Materials Science Forum, 551-552, 2007, 287-292.
6. Cheong B.H., Lin J. and Ball A.A. Modeling of the hardening characteristics for superplastic materials. Journal of Strain Analysis for Engineering Design, 35(3), 2000, 149-157.
7. Clarke D.R., Suresh S. and Ward I.M. (Eds.) Superplasticity in metals and ceramics. Cambridge University Press, 1997.
8. Dunne F. and Petrinic N. Introduction to Computational Plasticity. Oxford University Press, 2005.
9. Dziubińska A., Majerski K., Winiarski G. Investigation of the effect of forging temperature on the microstructure of grade 5 titanium ELI. Advances in Science and Technology Research Journal, 11(4), 2017, 147-158.
10. Fan W. Flow behavior and microstructural evolution during superplastic deformation of AA8090 aluminium-lithium Alloy. PhD thesis, 1998.
11. Galiyev A. and Kaibyshev R. Superplasticity in a magnesium alloy subjected to isothermal rolling. Scripta Materialia, 51, 2004, 89-90.
12. Gomez-Gallegos A., Mandal P., Gonzales D., Zuelli N. and Blackwell P. Studies on Titanium Alloys for Aerospace Applications. Defect and Diffusion Forum, 385, 2018, 419-423.
13. Henshall C.A., Wadsworth J., Reynolds M.J. and Barnes A.J. Design and manufacture of a superplastic-formed aluminium-lithium component. Materials & Design, 8(6), 1987, 324-330.
14. Hosford W.F. and Caddel R.M. Metal forming: Mechanics and Metallurgy. 4th Edition. Cambridge University Press, 2011.
15. Kawasaki M. and Langdon T.G. Developing Superplasticity in Ultrafine-Grained Metals. Acta Physica Polonica a, 128(4), 2015, 470-478.
16. Kharchenko V.V. Viscoplastic models in simulation of high strain-rate behavior of materials. Strength of Materials, 34(3), 2002, 219-222.
17. Khraisheh M., Zbib H., Hamilton C. and Bayoumi A. Constitutive modeling of superplastic deformation. Part I: Theory and experiments. International Journal of Plasticity, 13(1-2), 1997, 143-164.
18. Kotov A.D., Mikhailovskay A.V., Mosleh A.O., Pourcelot T.P., Prosviryakov A.S. and Portnoi V.K. Superplasticity of an Ultrafine-Grained Ti-4% Al-1% V-3% Mo Alloy. Physics of Metals and Metallography, 120(1), 2019, 60-68.
19. Langdon T.G. Thirty Years of Superplastic Ultrafine-Grained Materials: Examining the Legacy of Oscar Kaibyshev. Defect and Diffusion Forum, 385, 2018, 3-8.
20. Lin J. and Dunne F.P.F. Modelling grain growth evolution and necking in superplastic blow-forming. International Journal of Mechanical Sciences, 43(3), 2001, 595-609.

21. Lin J. and Yang J. GA-based multiple objective optimisation for determining viscoplastic constitutive equations for superplastic alloys. International Journal of Plasticity, 15(11), 1999, 1181-1196.
22. Majidi O., Jahazi M. and Bombadier N. Finite Element Simulation of High-Speed Blow Forming of an Automotive Component. Metals, 8(11), 2018, 1-12.
23. Majidi O., Jahazi M. and Bombardier N. A viscoplastic model based on a variable strain rate sensitivity index for superplastic sheet metals. International Journal of Material Forming, 12(4), 2019, 693-702.
24. Mosleh A., Mikhaylovskaya A., Kotov A., Pourcelot T. , Aksenov S., Kwame J. and Portnoy V. Modelling of the Superplastic Deformation of the Near-α Titanium Alloy (Ti-2.5Al-1.8Mn) Using Arrhenius-Type Constitutive Model and Artificial Neural Network. Metals, 7(12), 2017, 1-15.
25. Mosleh A.O., Mikhaylovskaya A.V., Kotov A.D. and Kwame J.S. Experimental, modeling and simulation of an approach for optimizing the superplastic forming of Ti-6%Al-4%V titanium alloy. Journal of Manufacturing Processes, 45, 2019, 262-272.
26. Mukai T., Wanatabe H. and Higashi K. Application of superplasticity in commercial magnesium alloy for fabrication of structural components. Materials Science and Technology, 16(11-12), 2013, 1314-1319.
27. Muthusamy B. and Ramanathan K. Numerical simulation and analysis of superplastic forming in Ti-6Al-4V alloy. International Journal of Applied Engineering Research, 55(10), 2015, 3746-3750.
28. Nieh T.G., Wadsworth J. and Sherby O.D. Superplasticity in metals and ceramics. Cambridge University Press, 1997.
29. Oh-ishi K., Boydon J. and McNelley T.R. Processing, deformation, and failure in superplastic aluminum alloys: Applications of orientation-imaging microscopy. Journal of Materials Engineering and Performance, 13(6), 2004, 710-719.
30. Padmanabhan K.A., Vasin R.A. and Enikeev F.U. Superplastic flow: Phenomonology and Mechanics. Springer-Verlag, 2001.
31. Patel V.V. and Badheka V. Influence of Friction Stir Processed Parameters on Superplasticity of Al-Zn-Mg-Cu Alloy. Materials and Manufacturing Processes, 31(12), 2015, 1573-1582.
32. Pozdniakov A.V., Barkov R.Y., Amer S.M., Levchenko V.S., Kotov A.D. and Mikhaylovskaya A.V. Microstructure, mechanical properties and superplasticity of the Al-Cu-Y-Zr Alloy. Materials Science and Engineering A, 758, 2019, 28-35.
33. Prasad N.E. and Wanhill R.J.H. Aerospace Materials and Material Technologies. Volume 2: Aerospace Material Technologies. Springer, 2017.
34. Prasad N.E., Gokhale A.M. and Wanhill R.J.H. Aluminum-Lithium Alloys. Processing, Properties and Applications. Elsevier, 2014.
35. Rajasekaran A., Sundar Singh Sivam S.P., Rajendrakumar S. and Saravanan K. Influence of setting variables in conventional super plastic forming process using grey relation analysis in taguchi method. ARPN Journal of Engineering and Applied Science, 12(15), 2017, 4648-4655.
36. Ridley N. Metals for superplastic forming, in: G. Giuliano, (eds.) Superplastic forming of advanced metallic materials. Woodhead Publishing, 2011.
37. Ridley N. Superplastic Forming and Diffusion Bonding of Titanium Alloys, in: R. Blockley, (eds.), Encyclopedia of Aerospace Engineering, John Willey & Sons, 2010.
38. Sherby O.D. and Burke P.M. Mechanical behavior of crystalline solids at elevated temperature. Progress in Materials Science, 13, 1968, 323-390.
39. Sherby O.D. and Wadsworth J. Superplasticity – Recent advances and future directions. Progress in Materials Science, 33(3), 1989, 169-221.
40. Sieniawski J. and Motyka M. Superplasticity in titanium alloys. Journal of Achievements in Materials and Manufacturing Engineering, 24(1), 2007, 123-130.
41. Tully K. and Monaghan J. Bulk forming of superplastic alloys. Journal of Materials Processing Technology, 26(2), 1991, 159-171.
42. Vasin R. A. and Filippov O.G. On Dependence of the Stress on Strain Rate of Superplastic Materials. Strength of Materials, 32(4), 2000, 311-315.
43. Vasin R. A., Berdin V. K. and Kashaev R.M. On the Universal Curve in Superplasticity Mechanics. Strength of Materials, 33(6), 2001, 509-515.
44. Wang J., Verma S., Alexander R. and Gau J.T. Springback control of sheet metal air bending process. Journal of Manufacturing Processes, 10, 2008, 21-27.
45. Winowiecka J. The analysis of springback of titanium sheet after bending. Obróbka Plastyczna Metali, 24(3), 2013, 219-232.
46. Wu L.H., Jia C.L., Han S.C., Li N., Ni D.R., Xiao B.L., Ma Z.Y., Fu M.J., Wang Y.Q. and Zeng Y.S. Superplastic deformation behavior of lamellar microstructure in a hydrogenated friction stir welded Ti-6Al-4V joint. Journal of Alloys and Compounds, 787, 2019, 1320-1326.
47. Yu H., Yan M., Li J., Godbole A., Lu C., Tieu K., Li H. and Kong C. Mechanical properties and microstructure of a Ti-6Al-4V alloy subjected to cold rolling, asymmetric rolling and asymmetric cryorolling. Materials Science and Engineering: A, 710(5), 2018, 10-16.
48. Zhao L., Yasmeen T., Gao P., Wei S., Bai Z., Jiang J. and Lin J. Mechanism-based constitutive equations for superplastic forming of TA15 with equiaxed fine grain structure. Procedia Engineering, 207, 2017, 1874-1879.